A Precision Grinding Technology for Zirconium Alloy Tubes Based on Ultrasonic Wall Thickness Automatic Measurement System

Lai Zou
Chongqing University
Heng Li
Chongqing University
Wenxi WANG (wx.wang@cqu.edu.cn)
Chongqing University https://orcid.org/0000-0001-8467-2530
Yun Huang
Chongqing University
Yutong Li
Chongqing University

Research Article

Keywords: Ultrasonic, Zirconium alloy, Wall thickness, Measurement, Tubes, Grinding

Posted Date: December 30th, 2021

DOI: https://doi.org/10.21203/rs.3.rs-1155325/v1

Abstract

To ensure the safety and long-term performance of nuclear fuel cladding zirconium tubes, the wall thickness uniformity of each cross section is strictly needed. Therefore, this paper presents comprehensive investigations on development of an automatic ultrasonic wall thickness measurement system for detecting the nuclear zirconium tubes. Based on the determination of overall scheme, optimization of key mechanical structures and design of control system, a series of performance testing analyses of this developed auto-measuring system were performed from aspects of measuring accuracy, measuring efficiency, stability and practicability. The results revealed that it could accurately obtain the wall thickness distribution and effectively guide the subsequent grinding process by automatically generated deviation correcting procedures to achieve the requirement of the wall thickness uniformity. The new combination method of ultrasonic auto-measuring and numerical control grinding proposed in this work would have a great significance for the development and application of nuclear reaction zirconium alloy container.

1. Introduction

Zirconium alloys have been widely used for fuel cladding and core structure components in water-cooled nuclear reactor owing to its excellent mechanical and physicochemical properties. Such as low thermal neutron absorption cross-section, high thermal conductivity, favorable corrosion resistance and compatibility with nuclear fuel [1-4]. Nuclear fuel cladding zirconium tube is considered as the first safe line of defense in the nuclear power plant, therefore the demands for wall thickness uniformity of cross sections and the surface quality of zirconium alloy tubes during a series of processing have increased markedly in recent years [5-7]. In addition, the adverse working conditions (high temperature and high pressure, neutron radiation and iodine vapor corrosion) will result in the localized corrosion damages of the tubes and abnormal operation of the nuclear power plant, even causing a nuclear leakage [8-14]. Thus considerable attention should be paid to a suitable measuring method to primarily assure the uniform wall thickness of cross sections in the processing of zirconium alloy tubes.

Currently, a large number of measuring methods have been performed to obtain the wall thickness distributions of different kinds of tubes in industrial fields. For instance, eddy current measuring, magnetic flux leakage measuring, laser measuring and X-ray measuring [15, 16]. Compared with these detecting techniques, the ultrasonic measuring method showed a great potential in detecting of the nuclear tubes as a result of its good directionality, strong penetrating power, high sensitivity, and non destructiveness, etc [17-19]. Although considerable researches have been devoted to ultrasonic measuring of the tube wall thickness in nuclear industry field, rather less attention has been paid to the ultrasonic measurement of the wall thickness of the zirconium alloy tube blank. Especially, the most of previously mentioned investigations were performed based on a continuous thickness gauge in the light of point by point manual measuring method, which would give rise to the detection efficiency and accuracy were difficult to guarantee. More importantly, the forementioned work were lack of a systematic

study on effectively guiding the subsequent precision processing by the wall thickness measurement results [20].

In consideration of the subsequent processing, consequently, an ultrasonic wall thickness auto-measuring system of the nuclear fuel cladding zirconium alloy tube was developed in this work, and then confirmed by means of a series of the system performance testing analyses. It was used to accurately obtain the wall thickness distribution of each cross section and effectively guide the abrasive machining of zirconium tubes.

2. Development Of Measurement System

2.1 Overall scheme design

Figure 1 shows the complete processing procedures of the nuclear fuel cladding zirconium tubes. For the sake of ensuring the wall thickness uniformity of the tubes and improving the utilization of Pilgering cold rolled link, in this work, the development of an ultrasonic measuring system and the subsequent grinding process guided by the measuring results formed the wall thickness measuring and grinding part marked by the red circle as shown in this figure.

Figure 2 displays the common surface flaws of the Zr-4 alloy tubes used in this work. It could be obviously seen that a large number of defects emerged on the internal and external surfaces of the tube after a series of abovementioned technological processing. In addition, the external surface was covered by a dense layer of oxide film. Although the surface quality of the zirconium tube could be greatly improved after the abrasive machining, a few defects would still exist due to guarantee the machining efficiency in actual production. Thus it was primarily required that the developed measuring system should have the ability to adapt to these defects to a certain degree.

Even worse, the hot extrusion and other technological processes would lead to the severe axial deformation, the floating radial dimension and the poor straightness of zirconium alloy workpieces, so that the wall thickness distributions of cross sections were nonuniform.Therefore it was required that the measuring system should have the ability to be adaptive to offset the deformation, in order to prevent ultrasound from contacting with air for improving the measuring accuracy.

On basis of actual production experiences about the subsequent cold rolling process, the wall thickness uniformity of the cladding tube products could be effectively ensured as the wall thickness deviation of each cross section is less than 0.38 mm in the current link [21, 22]. In view of the certain deviations derived from the grinding process, the allowable deviations of measuring and grinding are respectively set as 0.08 mm and 0.11 mm, in order to assure the working accuracy and working efficiency of each procedure. Table 1 shows the main technical parameters of the preliminary designed measuring system in consideration of the practically applied requirements.

Table 1. Main technical parameters of measurement system

Parameters	Values
Measuring range of diameter (mm)	60-90
Measuring range of wall thickness (mm)	0.1-30
Measuring range of length (m)	2.5-5
Measuring accuracy (mm)	0.01
Spindle speed (r/min)	1-300
Axial feed rate (m/min)	0-8

2.1.1 Ultrasonic measurement principle

The frequently-used ultrasonic thickness measuring techniques are mainly divided into resonance, penetration and pulse reflection type based on different measurement principles. By comparison, the ultrasonic pulse reflection mode was selected in this measuring system because of its high sensitivity, high positioning accuracy and convenient operation. The wall thickness of zirconium tube was obtained by recording the propagation time of ultrasonic pulse in the workpiece material back and forth. It could be calculated by the equation as follows.

$$d = \frac{1}{2} c \Delta t \qquad (1)$$

where d is the wall thickness of the tube blank, Δt is the propagation time of the ultrasonic wave in the workpiece back and forth, and c is the propagation velocity of ultrasonic wave in the workpiece material.

2.1.2 Ultrasonic measurement pattern

For the sake of reducing the effect of workpiece vibration and rotation on ultrasonic propagation path, a specific ultrasonic measuring pattern with regard to the relative motion relationship between the tube and ultrasonic probe was proposed in this work. The workpiece rotated intermittently while the probe remained stationary in the detection of one cross section, then the probe was shifted to the next section.

Taking the measuring accuracy and efficiency into account, several cross sections were selected uniformly-spaced on the tube and the detection points were selected with equal angle. The specific ultrasonic measuring pattern was shown in Figure 3. It was worth noting that the selection principle of cross section spacing l and the number of detection points n were based on the measured results could reliably represent the wall thickness distribution of entire tube.

2.1.3 General scheme of ultrasonic measurement

As shown in Figure 4, it can be seen that the whole framework of measuring system was mainly composed of the following parts: signal transmission and reception, signal processing section, data processing section, control system and operating section, etc. High speed network communication bus

was used as the system information transmission bridge and the industrial personal computer was used as the upper monitor of data processing in this thickness measuring system. On the basis of applying programmable logic controller (PLC) to realize the relative motion between ultrasonic probe and workpiece, the wall thickness measurement of zirconium alloy tube could be ultimately achieved through the emission and reception of ultrasonic signals, high-speed sampling and signal processing.

Figure 5 reveals the concrete structure scheme of measurement system. It can be seen that the wall thickness measuring device was fixedly connected on the grinding head of deviation correcting device, and the axial movement of ultrasonic probe in different cross sections was controlled by X-axis servo motor, which was used to drive the grinding head translation. Besides, the workpiece clamping device was shared to eliminate the benchmark misalignment error arose from the repeated positioning in measurement link and deviation correction link. During measuring process, rotation of the located and clamped workpiece was driven by A-axis servo motor in accordance with the designated angle. Subsequently PLC was used to drive the overflow box with probe installed on the cylinder down to the workpiece, and the coupling agent was supplied to eliminate air in overflow box while it closely contacted with the workpiece. Finally, the ultrasonic wave was transmitted to measure the tube wall thickness.

With completion of the wall thickness measuring in the current cross section, the overflow box was lifted by the shrinking cylinder and the ultrasonic probe as well as the grinding head would be moved to the next section by X-axis servo motor. Repeating the above steps until the measured data would be storage and displayed to successfully prepare for the next step of wall thickness deviation correcting.

2.2 Mechanical structure design

In consideration of the relative motion relationship between the measured tube and ultrasonic probe, as well as the close relationship between wall thickness measuring system and deviation correcting device, the particular attention should be paid to optimized design of the following key mechanical structures of this ultrasonic measuring system.

2.2.1 Probe moving

Figure 6 depicts the three-dimensional model of ultrasonic probe moving part. It was used for adjusting the probe position and controlling the overflow box down to the workpiece in the process of measuring, so as to ensure a good fit between the workpiece and seal block. On account of the position accuracy of the ultrasonic probe would directly affect the characteristics of ultrasonic wave emitted by probe and the detection capability of ultrasonic echo, so several connected hinges were designed in this device for neatly achieving the three-coordinate motion of the probe, additionally ensuring the probe perpendicular to the front surface of the workpiece.

2.2.2 Overflow

The overflow part was mainly composed of the overflow box and seal block, it was applied to adjust the depth of coupling agent between probe and workpiece as well as leading the outflow of excess coupling

agent [23]. The overflow type of partial immersion was adopted in this work to form an acoustic coupling between the measured workpiece and overflow surface. It can be seen that a large hole of the lower end was used to feed and four evenly distributed small holes of the upper end were used to overflow in this designed overflow box as shown in Fig.7(a). The probe was always immersed in the coupling agent under the condition of adequate flowing and good sealing, which could effectively ensure the normal transmission and the reception of ultrasonic signals. The water depth between the probe and coupling agent was obtained by multiple coincidence method with the calculation equation shown in the following.

$$H = \frac{C_{l1}}{C_{l2}} Tn \tag{2}$$

where H is the water depth between the probe and coupling agent, T is the wall thickness of zirconium tube, n is the coincidence frequency, C_{l1} and C_{l2} are the longitudinal wave velocity in water and in workpiece material respectively. The adjusting nut seen in Fig.7(a) was used to drive the probe up and down for regulating the water depth in measuring workpiece with different sizes. To meet the performance requirements of this ultrasonic measuring system, the water depth H was calculated by the above formula for 20 mm in current conditions.

For ensuring the sealability of coupling agent and improving the measurement accuracy of developed system, the designed seal block was shown in Fig.7(b). The large circular hole in the center of seal block was used for positioning and installing of the probe. The ultrasonic signal could be well separated from the air by means of a flexible polymer sealing strip which could be automatically attached to the workpiece surface. Moreover, the wall thickness could still be measured when a certain deviation emerged between actual size and theoretical size of the workpiece because of the elastic property of polymer sealing strip, also the measurement of workpieces with different external diameters could be achieved by changing the size of seal block. Figure 7(c) shows the physical structure of the probe moving part and overflow part. Not only did this device have good sealing performance, but also it was good to meet the process requirements of quick conversion from the auto-measuring measurement to the wall thickness deviation correcting.

2.2.3 Workpiece clamping and driving

The measured zirconium alloy tube was positioned and clamped by the double centres and partly immersed in the coupling agent. The active centre was driven by A-axis servo motor to achieve measuring with equal angular spacing, and the follower centre was driven by cylinder to clamp the workpiece. Unlike the equidistant measurement of different interfaces was controlled by X-axis servo motor. The diameter and length of the workpiece were measured in a range of 60 mm to 90 mm, and 2.5 m to 5 m respectively for this designed device.

2.2.4 Couplant supplying

From the point of view of the acoustic transfer characteristic, enough infiltration of the fluid couplant was required to eliminate the air gaps caused by the rough surface between probe and workpiece. In addition, its acoustic characteristic impedance was close to the specimen as possible to increase the ultrasound energy transferred into the workpiece [24]. The shared supplying mode of coupling agent and grinding fluid was adopted in the work, and the details of the supply process were shown in Figure 8. It can be seen that the grinding fluid extracted by water pump was shunted into two strands of liquid. One was sent to the overflow box as a coupling agent to meet the requirements of the probe and workpiece, the other was transferred to the grinding head to play a role of coolant in wall thickness correction link. Both coupling agent and grinding fluid eventually converged into the clean liquid through once paper-based filtering and twice precipitation filtration. This couplant supplying model was in line with the requirements of current green and sustainable manufacturing.

2.3 Control system design

Figure 9 illustrates the PLC installation layout mode of the electric control system in this work. It was used to control of the important movements of developed device, such as localization and translation of the probe, the workpiece clamping and rotating, the overflow box pressed down and lifted up. Further completing the control of data acquisition, data processing and data storage, to achieve the wall thickness measurement of zirconium alloy tube and provide guidance for the subsequent grinding process.

2.3.1 Data acquisition

The transmission and acquisition of signals were performed by ultrasonic card ZXUS-PC4 and its main technical parameters were shown in Table 2. The monitor software was utilized for measuring the ultrasonic velocity, adjusting the waveform and setting the parameters of detected materials. Then the initialization of ultrasonic signals and acquisition of ultrasonic data were realized by the programming technique. The liquid immersion flat ultrasonic probe with a diameter of 12 mm was selected with the emission frequency was 50 KHz.

Table 2. Main technical parameters of ZXUS-PC4 ultrasonic card

Technical parameters	Value
Sampling frequency (MHz)	100
Sound velocity (m/s)	250-16000
Resolution ratio (dB)	≥40
Transmission gain (dB)	0.1
Emission pulse width (ns)	50-500
Emission delay (us)	0-400

2.3.2 Data processing

Figure 10 demonstrates the determination principle of the section numbers for zirconium tubes. The probe center was used as the positioning standard during measuring process and the cross section was taken at intervals of l from the reference point in the system. The number of cross sections was calculated by the following formula to obtain a favorable sealing performance, where l_1 was the length of the seal block.

$$(m-1)\times l+(l_1/2)\times 2\le L \tag{3}$$

Based on the measuring pattern of workpiece rotating and probe translating intermittently, the data processing strategy was divided into two cases of the same section and different sections in order to take account of the measuring efficiency and measuring accuracy synthetically.

On the same cross section, all the tested points were repeatedly measured three times. Assuming that the data of a detection point was a, b and c ($a>b>c$), the measured result of this point was defined as β, and the critical value Δ of deviation was set to 0.08mm for judging whether the data was abnormal in this system. The final wall thickness measuring result of detection point was determined by the following formula. Furthermore, all the measured data of this cross section was judged to be invalid if more than tenth measured data in the same section was abnormal.

$$\begin{cases} a-c\le\Delta,\ \beta=(a+b+c)/3 \\ a-c>\Delta\begin{cases} a-b>\Delta\begin{cases} b-c>\Delta,\ \beta=\text{invalid} \\ b-c\le\Delta,\ \beta=(b+c)/2 \end{cases} \\ a-b\le\Delta\begin{cases} b-c>\Delta,\ \beta=(a+b)/2 \\ b-c\le\Delta\begin{cases} a-b\le b-c,\ \beta=(a+b)/2 \\ a-b>b-c,\ \beta=(b+c)/2 \end{cases} \end{cases} \end{cases} \end{cases} \tag{4}$$

On the different cross sections, the wall thickness distributions of two adjacent sections were approximately the same, thus the data processing program of different sections could be divided as follows.

Strategy 1. If a large number of inaccurate data appeared in one of the middle cross sections, the average value of the corresponding point of the two adjacent cross sections would be taken as the wall thickness value of this section.

Strategy 2. If a large number of inaccurate data appeared in the first cross section, stopping the program and eliminating the other reasons, and then continued to measure.

Strategy 3. If a large number of inaccurate data appeared in the last cross section, the measured data of reciprocal second cross section would be taken as the wall thickness value of this section.

Strategy 4. If a large number of inaccurate data continuously appeared in two adjacent cross sections, the system would alarm and stop detection, then restarting the system after a comprehensive check.

2.3.3 Data storage

The wall thickness measured data was displayed in two forms. To facilitate the processing and calculating of subsequent data, one was stored in the form of text and the detection results of one point were listed in sequence of sectional position, angular position, the average wall thickness and wall thickness deviation. However, this storage form could not directly show the distribution of wall thickness deviation of the whole zirconium tube. Especially, this problem was more prominent when the workpiece was longer. Therefore, the wall thickness deviation of whole workpiece was calculated and then plotted in the form of color histogram in this work. Figure 11 shows the distribution of wall thickness deviation in this storage form, the horizontal and vertical axes represented the axial and circumferential position of the detection points, respectively. On account of the critical value of deviation correction was defined as 0.38 mm as mentioned above, it can be seen that the wall thickness deviation correcting was required in the two areas circled by red line. Consequently, it was thus clear that this data storage form could directly and quickly determine the wall thickness deviation correcting areas, which were needed to be performed on the corresponding grinding with the accurate machining allowance.

3. Experimental Verification Of Measurement System

3.1 Measuring accuracy

Measuring accuracy was one of the important indicators to judge the reliability and accuracy of developed system. Hence a high precision Olympus hand-held ultrasonic thickness gauge and this developed auto-measuring system were respectively used to measure the wall thickness for the same zirconium alloy tube with no obvious defects. Figure 12 shows the wall thickness measuring curves of two arbitrary selected sections of the identical workpiece obtained by these two ways. It can be evidently seen that the deviation of measurment results between ultrasonic auto-measuring and manual measuring was about 0.01 mm, except for the deviation of twentieth points in the cross section No.1 was 0.03 mm. Therefore, the measurement accuracy of this developed system could be approximately determined as 0.01 mm in current conditions.

3.2 Measuring efficiency

The main factors affecting the detection efficiency were workpiece rotating velocity w, number of detection points in one cross section n and distance between adjacent cross sections l. The time t used for detection of a single section was obtained in Table 3 under the combination of different parameters in condition of the spacing of adjacent cross sections was set to 100 mm. It could be deduced that the time used for detection of individual section would be reduced with the increment of workpiece rotating speed and the reduction of number of detection points. In comprehensive consideration of the requirements of measuring accuracy and efficiency, the detection efficiency standard determined as time-consuming of

each section was 1’47”, which was improved by nearly 3 times compared with the working efficiency of manual measurement.

Table 3. Measuring efficiency in different combination of *n* and *w*

w(rpm) *n*	20	30	40	50
15	1’51”	1’33’	1’30”	1’22”
20	2’05”	1’45”	1’40”	1’33”
24	2’11”	1’55”	1’47”	1’44”
30	2’27”	2’11”	2’05”	2’01”

3.3 System stability

Two nuclear fuel cladding zirconium tubes without any obvious surface defect were selected in these tests, and the measured consistency of two repeated detecting for each workpiece was used to evaluate the system stability. The detailed detection parameters of workpieces were shown in table 4.

Table 4. Detailed detection parameters of two workpieces

	Workpiece No.1	Workpiece No.2
Length×diameter (mm×mm)	86×3750	86×3900
Number of cross sections	26	27
Section spacing (mm)	150	150
Total number of detection points	624	648

Figure 13 describes the wall thickness morphology of repeated detecting for each workpiece based on the measured results. It can be seen that the wall thickness profile obtained by two measurements was basically the same except slight difference existed in the local areas. By subtraction of the two groups of measured wall thickness data, the maximum difference between the two measuring values at the same point was less than 0.03 mm. Moreover, it could be deduced that the measuring process was well sealed and stable from the smooth graphics surface. Therefore, these were enough to prove that the developed auto-measuring system was reliable.

3.4 System practicability

As mentioned above, if the wall thickness distribution of zirconium tube acquired by this ultrasonic measuring system was not satisfied with the deviation request, it was necessary to conduct the following grinding process. Hence the wall thickness of two zirconium tubes with different diameters (86 mm and 64 mm) were measured before and after the grinding, it was worth noting that the allowable deviation of

wall thickness was 0.38 mm and 0.30 mm, respectively. Figure 14 presents the wall thickness deviation of zirconium tubes before and after the correcting. It can be obviously seen that these two workpieces were not satisfied with the requirement of wall thickness deviation before correcting. However, the maximum wall thickness deviation of workpiece No.3 and No.4 were about 0.28 mm and 0.22 mm respectively after numerical control grinding, which were both meet the deviation requirement. Therefore, the measuring accuracy and practicability of this system were indirectly proved by these experimental results.

In order to further verify the practicability of developed system, the wall thickness of nuclear fuel cladding zirconium tube was measured and polished by the combination of ultrasonic auto-measuring and numerical control grinding method. Figure 15 visually displays the change of surface quality before and after grinding based on the measured results. It could be distinctly deduced that this measuring system had an important guiding role for the subsequent wall thickness correcting. Additionally, this new combination method could effectively improve the wall thickness distribution and manufacturing accuracy of the zirconium alloy tubes.

4. Conclusion

In this present work, a series of comprehensive investigations on the development of an ultrasonic auto-measuring system have been performed to solve the issue about the strict uniformity requirements for the wall thickness of zirconium alloy tubes. The main conclusions obtained were summarized as follows.

(1) A suspension type and partial liquid-immersed ultrasonic auto-measuring system was developed to accurately obtain the wall thickness distribution of zirconium tubes, further effectively guiding the subsequent grinding process by the deviation correcting procedure directly generated from the measured results.

(2) Comprehensive performance testing analyses were performed for this developed system from aspects of measuring accuracy, measuring efficiency, stability and practicability. The experimental results revealed that this system could commendably meet the requirements of wall thickness measuring. It was worth mentioning that both the deviation and uniform degree of wall thickness could achieve the corresponding objectives after numerical control grinding.

(3) The new combination method of ultrasonic auto-measuring and numerical control grinding proposed in this work would gradually replace the current manual measuring and manual polishing, as it could effectively improve the manufacturing accuracy of zirconium alloy tube and had an important significance for the development and application of nuclear reaction zirconium alloy container.

Declarations

Author contributions Lai Zou: funding acquisition, project administration, resources, and supervision. Heng Li: investigation, methodology, and writing original draft. Wenxi Wang: experiment, data, and

conceptualization. Yun Huang: equipment and software. Yutong Li: writing review and editing.

Funding This study was supported by the National Natural Science Foundation of China (Grant No. 52075059, 52105430) and the Natural Science Foundation of Chongqing (Grant cstc2020jcyj-msxmX0266).

Data availability statement Not applicable

Code availability Not applicable

Competing interests The authors declare that they have no known competing financial interests or personal relationships that could have appeared to influence the work reported in this paper.

Ethical approval Not applicable.

Consent to participate Not applicable.

Consent to publish Manuscript was approval by all authors for publication.

References

1. Li FS, Li SL, Yang K, Wang Y L (2021) Morphology and microstructure evolution of surface hydride in zirconium alloys during hydrogen desorption process. Int J Hydrog Energy 46(47): 24247-24255.
2. Zeng QH, Luan BF, Adrien C, Liu Q (2019) Evolution of crystallographic Texture of Zirconium Alloy During Hot Deformation. Rare Metal Mat Eng 48(8):2393-2399
3. Kim S, Rhyim Y, Kim J, Yoon J (2015) Characterization of zirconium hydrides in zircaloy-4 cladding with respect to cooling rate. J Nucl Mater 465: 731-736.
4. Cao JG, Wang T, Cao Y, Song CN, Gao B, Wang B (2021) Cold rolling force model of nuclear power zirconium alloy based on Particle Swarm Optimization. Int J Adv Manuf Technol 115:319-328.
5. Xu L, Xiao Y, Sandwijk AV, Xu Q, Yang Y (2015) Production of nuclear grade zirconium: A review. J Nucl Mater 466: 21-28.
6. Chen G, Zhang X, Xu DK, Li DH, Chen X, Zhang Z (2017) Multiaxial ratcheting behavior of zirconium alloy tubes under combined cyclic axial load and internal pressure. J Nucl Mater 86(23): 3595-3611.
7. Kim HG, Choi BK, Park JY, Jeong YH (2009) Influence of the manufacturing processes on the corrosion of Zr-1.1Nb-0.05Cu alloy. Corros Sci 51(10): 2400-2405.
8. Sun C, Yang ZB, Wu ZP (2018) Study on Corrosion Resistance of N36 Zirconium Alloy in LiOH Aqueous Solution. J Nucl Sci Technol 8(2): 101-104.
9. Qu J, Cooley KM, Shaw AH, Lu RY, Blau PJ (2016) Assessment of wear coefficients of nuclear zirconium claddings without and with pre-oxidation. Wear 356-357: 17-22.
10. Plyasov AA, Novikov VV, Devyatko YN (2021) A Review of Hydride Reorientation in Zirconium Alloys for Water-Cooled Reactors. Phys Atom Nucl 83(10): 1407-1424.

11. Yan CG, Wang RS, Wang YL, Wang XT, Bai GH (2015) Effects of ion irradiation on microstructure and properties of zirconium alloys-A review. Nucl Eng Technol 47(3): 323-331.
12. Tupin M, Bisor C, Bossis P, Chêne J, Bechade JL, Jomard F (2015) Mechanism of corrosion of zirconium hydride and impact of precipitated hydrides on the zircaloy-4 corrosion behaviour. Corros Sci 98: 478-493.
13. Xue XY, Bai XD, Tian ZY, Zhou QS, Liu JZ (2004) Nodular corrosion of zirconium alloys. Rare Metal Mat Eng 33(9): 902-906.
14. Cinbiz MN, Koss DA, Motta AT (2016) The influence of stress state on the reorientation of hydrides in a zirconium alloy. J Nucl Mater 477: 157-164.
15. Lebensohn RA, González MI, Tomé CN, Pochettino AA (1996) Measurement and prediction of texture development during a rolling sequence of zircaloy-4 tubes. J Nucl Mater 229: 57-64.
16. Benoit M, Bataillon C, Gwinner B, Miserque F, Orazem ME, Sánchez CM, Tribollet B, Vivier V (2016) Comparision of different methods for measuring the passive film thickness on metals. Electrochim Acta 201: 340-347.
17. Green R (2004) Non-contact ultrasonic techniques. Ultrason 42(1-9): 9-16.
18. Dixon S, Edwards C, Palmer SB (2001) High accuracy non-contact ultrasonic thickness gauging of aluminum sheet using electromagnetic acoustic transducers. Ultrason 39(6): 445-453.
19. Toshifumi K, Toru I, Wahidul W, Yasuyuki I, Toshiro I (2009) Evaluation of thermal sprayed coating using ultrasonic inspection by means of bottom echo back reflection. T Nonferr Metal Soc 19(4): 984-987.
20. Subramanian CV, Thavasimuthu M, Jayakumar T, Raj B (1997) Ultrasonic response of various types of code recommended reference defects-a comparative study. Int J Pres Ves and Pip 70(2): 97-101.
21. Murty KL, Charit I (2006) Texture development and anisotropic deformation of zircaloys. Prog Nucl Energ 48(4): 325-359.
22. Mani Krishna KV, Sahoo SK, Samajdar I, Neogy S, Tewari R, Srivastava D, Dey GK, Das GH, Saibaba N, Banarjee S (2008) Microstructural and textural developments during zircaloy-4 fuel tube fabrication. J of Nucl Mater 383(1-2): 78-85.
23. Youssef MH, Gobran NK (2002) Modified treatment of ultrasonic pulse-echo immersion technique. Ultrason 39(7): 473-477.
24. Shuttleworth P, Maupin J, Teitsma A (2005) Gas coupled ultrasonic measurement of pipeline wall thickness. J Pres Ves Technol 127(3): 290-293.

Figures

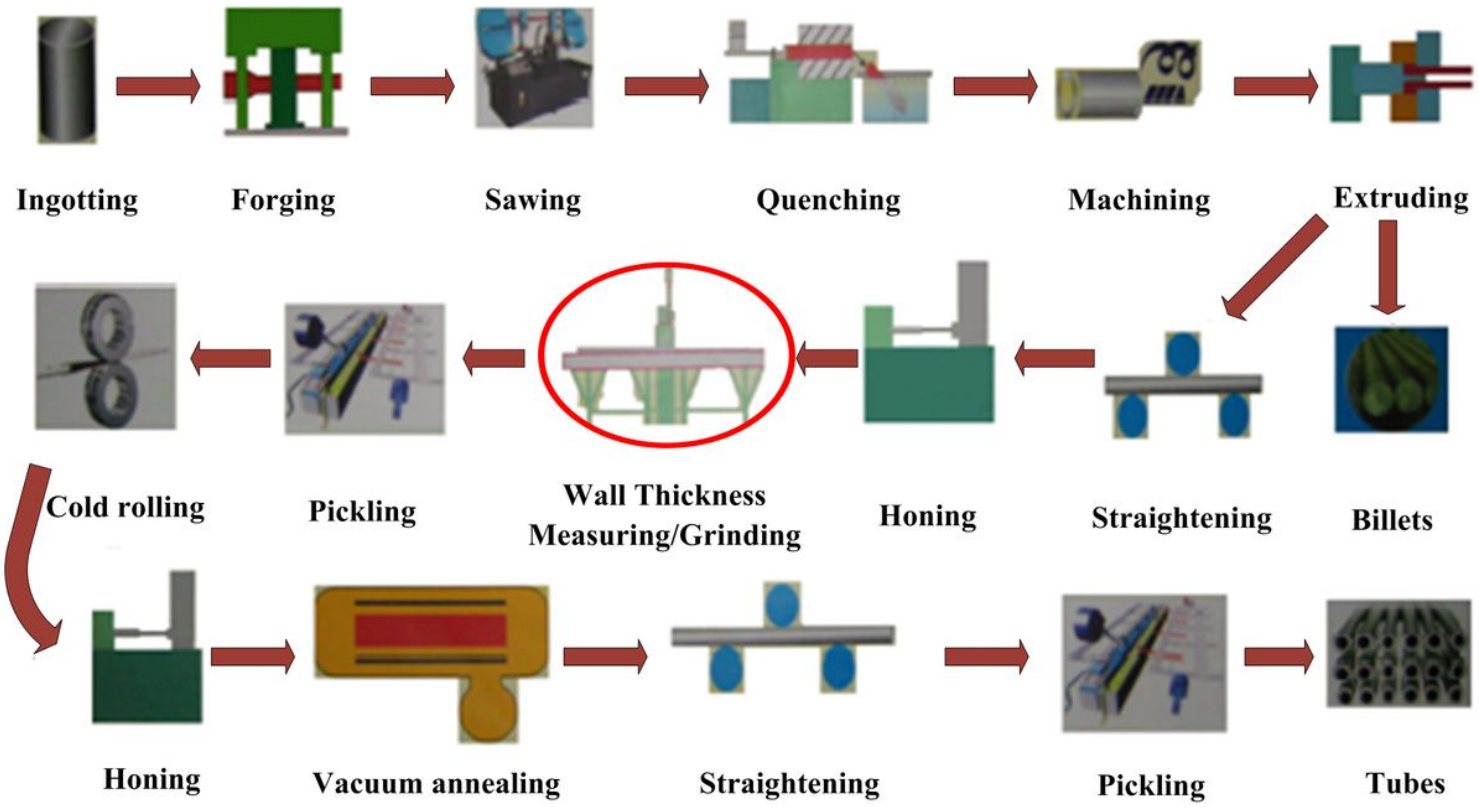

Figure 1

Processing procedures of the nuclear fuel cladding zirconium tubes

Figure 2

Common surface flaws. (a) Convex dges; (b) Oxidation films; (c) Grooves.

Figure 3

Specific ultrasonic measurement pattern of the system

Figure 4

Overall framework of the measurement system

Figure 5

Schematic diagram of three-dimensional structure of the developed system

Figure 6

Three-dimensional model of the probe moving part

Figure 7

Designed overflow part. (a) Overflow box; (b) Seal block; (c) Physical structure

Figure 8

Supply pattern of the coupling agent

Figure 9

PLC installation layout mode of the electric control system

Figure 10

Determination principle of the section numbers

Figure 11

Color histogram of the wall thickness deviation

Figure 12

Comparison of the obtained measuring results. (a) Section No.1; (b) Section No.2

Figure 13

Comparison of the wall thickness morphology in two repeated measurements. (a) Workpiece No.1; (b) Workpiece No.2

Figure 14

Wall thickness deviations of zirconium tubes before and after correcting. (a) Workpiece No.3; (b) Workpiece No.4

Figure 15

Changes of machined surface quality before and after grinding. (a) Before polishing; (b) During polishing; (c) After polishing